ENDOR analysis of the microscopic structures of the thermally driven bistable configurations of $F_H(OH^-)$ centres in KBr

1993 J. Phys.: Condens. Matter 5 1957

(http://iopscience.iop.org/0953-8984/5/13/012)

J. Phys.: Condens. Matter 5 (1993) 1957–1974. Printed in the UK

ENDOR analysis of the microscopic structures of the thermally driven bistable configurations of $F_H(OH^-)$ centres in KBr

H Söthe†, J-M Spaeth† and F Lüty‡

† Fachbereich Physik, University of Paderborn, Warburger Strasse 100, 4790 Paderborn, Federal Republic of Germany

‡ Physics Department, University of Utah, Salt Lake City, UT 84112, USA

Received 5 November 1992

Abstract. The aggregation of F centres and OH^- molecules to $F_H(OH^-)$ centres in KBr leads to a very interesting optical and thermal bistability. The structures of the bistable $F_H(OH^-)$ centres were investigated by using optical and conventional detection of electron nuclear double resonance (ENDOR). The analysis of the ENDOR spectra of both $F_H(OH^-)$ configurations is presented. It is shown that in both bistable configurations the OH^- molecule resides on a next-nearest anion site (fourth shell). The bistable configurations differ in the orientation of the OH^- dipole with respect to the F centre. The thermal bistability is tentatively explained as being due to entropy changes with temperature.

1. Introduction

F_H centres in alkali halides are aggregate centres between F centres and anion impurities. Of particular interest are F_H centres with molecular impurity anions, especially the $F_H(OH^-)$ centres (Baldacchini *et al* 1989, Gomes and Lüty 1984). Optical investigations of these centres in additively coloured and highly OH^- doped KBr crystals lead to the observation of centres exhibiting a novel optical and thermal bistability.

After aggregating the F centres by bleaching the F band in an OH^- doped KBr crystal at about 240 K a new absorption band due to the $F_H(OH^-)$ centres appears slightly red shifted compared to the F band. Upon cooling the sample to 4.2 K the absorption band shifts to the 'blue' (high-energy) side of the F absorption. This absorption is due to another centre configuration. Therefore we denote the centres at high temperatures as 'red centres' and those at low temperatures as 'blue centres'. Bleaching at low temperatures in the absorption of the blue centre leads to the absorption band observed at high temperature ('red centres'). At low temperatures red and blue centres can be converted and reconverted in a stable and reversible way (Baldacchini *et al* 1989).

In KCl doped with OH^- a low-temperature switching between two bistable states could not be observed. The $F_H(OH^-)$ absorption band is for all temperatures between 310 K and 3.6 K red shifted compared to the F band.

The site of the OH^- ion relative to the F centre was not known in KBr. It could be either in a nearest (110) anion position (second shell) or in a next-nearest (200) anion position (fourth shell) as was found for the $F_H(OH^-)$ centres in KCl (Jordan *et*

0953-8984/93/131957+18$07.50

al 1988). Baldacchini *et al* (1989) speculated that the bistability is due to two different orientational configurations of the OH^- impurity relative to the F centre. It was the purpose of this work to determine the site of the OH^- as well as to determine the microscopic structures of the two bistable configurations by applying electron nuclear double resonance (ENDOR) techniques.

Söthe *et al* (1990) gave the first account of major results such as the centre models for the two bistable configurations and a discussion of the possible origin of the thermal bistability. In the present paper the details of the analysis of the ENDOR spectra of both defect configurations are presented as well as a full account of the superhyperfine (SHF) interaction constants determined experimentally. This presentation is followed by a short discussion of a possible explanation for the occurrence of the thermal bistability.

2. Experimental details

The KBr single crystals, doped with 2×10^{-2} and 1×10^{-2} mole fractions of KOH in the melt, were grown by the Czochralski method using Merck optipur and pro analysis materials. By additive colouration (Van Doorn 1961) F centre concentrations between 10^{16} and 10^{18} cm^{-3} were produced. Dark coloured samples were used for conventional electron spin resonance (ESR)/ENDOR experiments whereas samples with weaker colouration were preferred for optical and optically detected ENDOR (ODENDOR) experiments. When coloured samples are stored in daylight at room temperature, different types of F centre aggregates grow. Therefore the samples were quenched, i.e. they were heated to about 400 °C and then rapidly cooled to room temperature in the dark in order to produce isolated F centres. After this treatment the sample was mounted in the cryostat under weak red light.

The F centres were converted into $F_H(OH^-)$ centres at about 240 °C by bleaching the F centre absorption band. This process is analogous to the aggregation of F_A centres in alkali halides doped with impurity cations. As a light source for bleaching the F band a 150 W halogen lamp equipped with a 594 nm interference filter (Schott, NAL 594 nm) was used. The low-temperature conversions from blue into red centres and vice versa were performed by bleaching the blue or red centre absorption bands again with the 150 W halogen lamp and additional interference filters (PIL 579 nm, NAL 546 nm, NAL 653 nm and DAL 640 nm from Schott).

The ESR and stationary ENDOR experiments were performed with a custom-built computer-controlled X-band spectrometer (10 GHz). The sample temperature could be varied between 3.6 K (for a short time) and 300 K. The ENDOR frequency could be varied between 0.3 and 300 MHz. The ENDOR line positions were determined using digital filtering, deconvolution algorithms and a peak-search algorithm (Niklas 1983).

The optically detected ESR (ODESR)/ODENDOR spectrometer working in the K band (24 GHz) was also a custom-built computer-controlled system, using an Oxford bath cryostat and a 4 T supraconducting magnet. ODESR and ODENDOR experiments were usually performed at 1.6 K. Details of the spectrometer are described by Ahlers (1985).

The ODESR spectra were measured as microwave-induced changes of the magnetic circular dichroism of the absorption (MCDA) (Ahlers *et al* 1983). For the measurement of ODENDOR spectra with the MCDA technique (Hofmann *et al* 1984, Spaeth *et al* 1992) an additional radio frequency was simultaneously fed into the ODENDOR cavity.

3. ENDOR and ODENDOR results

Figure 1(*a*) shows the optical absorption spectra of F centres before aggregation and of the red and blue $F_H(OH^-)$ centres at 1.6 K. The red and blue shifts of the aggregate centres are clearly seen. The optical conversion between both $F_H(OH^-)$ configurations is so effective, that for the optically detected magnetic resonance (ODMR) measurements the measurement light had to be very weak. The peak to peak width of the derivative-like blue centre MCD is $\Delta E = (0.115 \pm 0.005)$ eV and that of the red centre (0.193 ± 0.005) eV (figure 1(*b*)). The blue centre absorption band and the MCDA both have an asymmetric low-energy tail. However, their true line forms cannot be determined, since the spectra of the centres overlap. The maxima of both absorption bands depend on the degree of conversion between the two $F_H(OH^-)$ centres; mixed states can also be observed. The line positions found for the best separation of the centres are at $E_{max} = (2.112 \pm 0.007)$ eV for the blue centre and $E_{max} = (2.017 \pm 0.007)$ eV for the red centre.

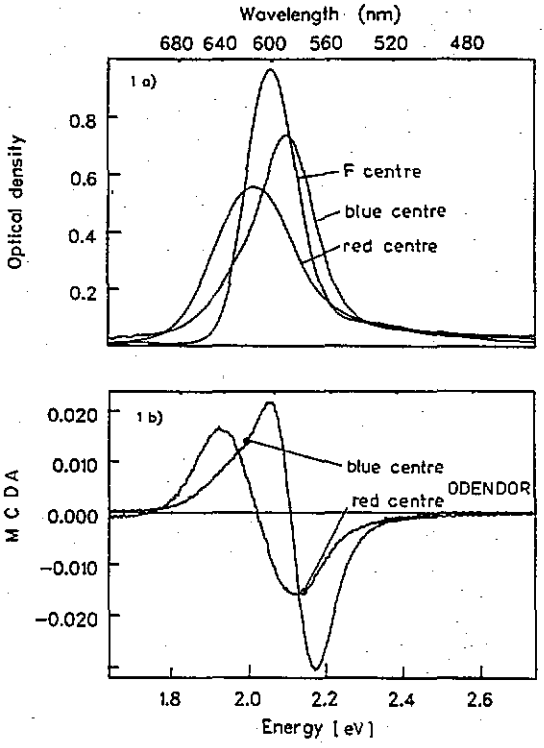

Figure 1. (*a*) Optical absorption of F centres and the red and the blue $F_H(OH^-)$ centres in KBr (KBr was doped with 2×10^{-2} KOH), $T = 1.6$ K. (*b*) Magnetic circular dichroism of the absorption of the red and blue $F_H(OH^-)$ centres in KBr. $B_0 = 875$ mT, $T = 1.6$ K. The circles show the wavelength where the ODENDOR of the blue and the red centres was measured (see text).

$F_H(OH^-)$ centres in KCl are red shifted compared to F centres and show only one absorption band (Gomes and Lüty 1984) and a derivative-like MCDA (Jordan 1987).

ODENDOR measurements of the ground state of the red and blue $F_H(OH^-)$ centres were performed using the MCDA technique (Spaeth *et al* 1992, Hofmann *et al* 1984). Compared to conventional ENDOR this detection method has the advantage that a direct correlation between the optical absorption band of a paramagnetic centre

and its ESR/ENDOR lines can be obtained (Hofmann *et al* 1984, Ahlers *et al* 1983). ODENDOR spectra measured before the F_H centre aggregation showed only known ENDOR lines of the isolated F centres (Seidel 1961). After formation of the $F_H(OH^-)$ centres the ODESR spectra measured throughout the MCDA showed no detectable difference in shape from the known ESR spectra of F centres in KBr. Only the broad unstructured ESR lines at $g = (1.97 \pm 0.02)$ with a half width of (17.5 ± 0.5) mT of the isolated F centre and those with half widths of (18.3 ± 0.5) mT for both $F_H(OH^-)$ centres were observed.

However, upon measuring ODENDOR new features appeared. When measuring ODENDOR by setting the optical wavelength in the high-energy flank of the MCDA at 1.6 K and thus producing red centres, a new set of ENDOR lines appeared compared to the unperturbed F centres (see figure 2, middle trace), while another set of ENDOR lines was measured after optically flipping the red centres into blue ones (figure 2, upper trace). The ENDOR spectra clearly show that $F_H(OH^-)$ centres are different from the isolated F centres and that the red and blue centres are definitively due to difference F–OH^- configurations. In order to prevent a conversion between centres being caused by the measurement light, the ODESR/ENDOR experiments were performed on the blue centre by setting the measurement light in the low-energy flank of its MCDA ($\lambda = 620$ nm). To observe the red centre, the light was set to $\lambda = 580$ nm, i.e. in the high-energy flank of the MCDA of the red centre. Unfortunately no more ENDOR lines could be detected optically. It turned out that the observed ODENDOR lines are due to second-shell Br^- neighbours.

Between 3.6 K and 20 K we could also measure conventional stationary ENDOR spectra. At 3.6 K both the red and blue centres were present simultaneously. Upon simultaneous *in situ* illumination with light in the low-energy flank (640 nm) or high-energy flank (546 nm) the relative intensities of the ENDOR lines of the blue and

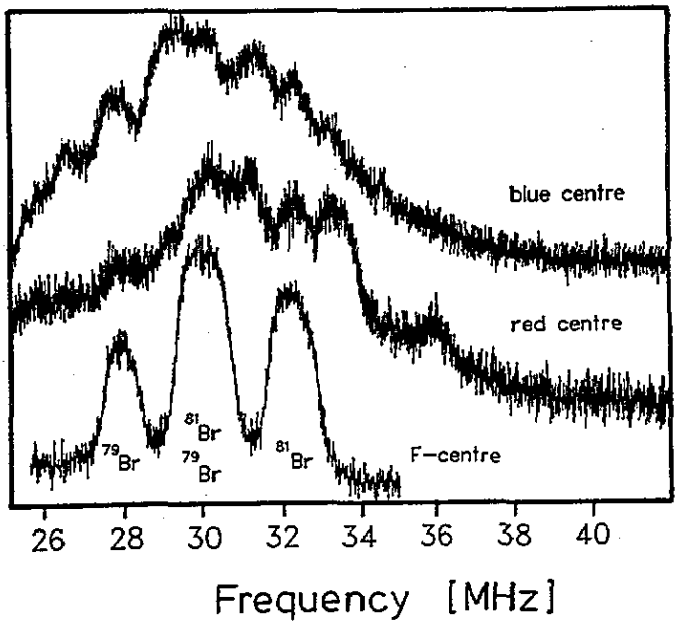

Figure 2. ODENDOR spectra of the isolated F centres and red and blue $F_H(OH^-)$ centres. $B_0 \| [100]$, $B_0 = 885$ mT, $T = 1.6$ K.

the red $F_H(OH^-)$ centres, respectively, could be changed significantly because of the optical switching between configurations.

In the ENDOR spectra observed at temperatures between 3.6 and 20 K the ENDOR lines of the blue and red $F_H(OH^-)$ centres are superimposed with those of the isolated F centres which were not aggregated to OH^- molecules. The ENDOR spectra containing $F_H(OH^-)$ centre lines were dominated by the more intense lines of F centres. Above 20 K the ENDOR lines of the $F_H(OH^-)$ centres vanished and only lines of the isolated F centres were measured. Figure 3 shows a typical ENDOR spectrum measured at 14 K. Some lines due to the blue and red centres are marked by arrows. The conventionally measured ENDOR lines have a much smaller line width than those detected optically and the interactions with both cation and anion neighbours as well as hydrogen atoms from the OH^- molecules could be resolved. For each orientation of the magnetic field numerous ENDOR lines were observed in the frequency range of 0.5–32 MHz. For the analysis the field orientation was varied in small angular steps of about 2°. Due to the overlays of the many ENDOR lines of the red, blue and isolated F centres (see also figure 3), the analysis of the ENDOR angular dependence was rather difficult. Some branches of ENDOR line sets were found by recognising the symmetry of the particular neighbours, when rotating the sample about its [001] axis.

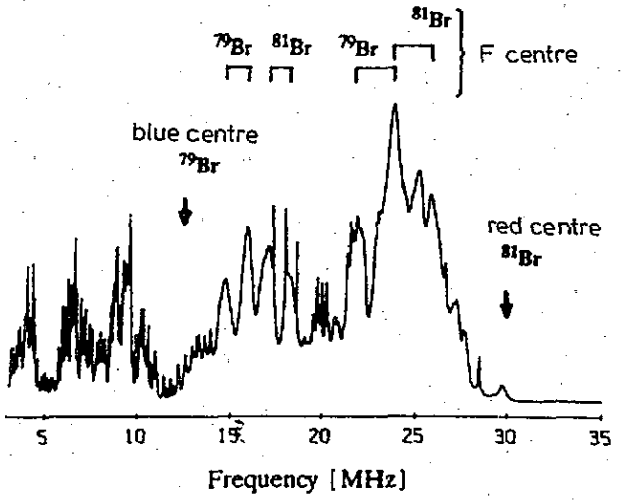

Figure 3. ENDOR spectrum of the $F_H(OH^-)$ centres in KBr. $B_0 \| [100]$. ENDOR lines due to the second-shell bromine neighbours of the isolated F centres and characteristic bromine lines of the blue and red centres are measured. $T = 14$ K, $B_0 = 342$ mT.

In principle the analysis of the ENDOR spectra and of the angular dependences measured for rotation of the magnetic field in a {100} plane proceeded along the lines described previously by Seidel (1961) for F centres. The chemical identity of the nuclei giving rise to ENDOR lines was determined with the field shift method (see also Spaeth *et al* 1992). The angular dependences were calculated using the appropriate spin Hamiltonian (Seidel 1961) and diagonalizing it numerically. The resulting SHF constants and the SHF tensor orientations are collected in table 1 for KBr and some data in table 2 for F and $F_H(OH^-)$ centres in KCl. The results are given in terms

of the isotropic SHF constants a and the anisotropic SHF constants b and b' and the quadrupole interaction constants q and q', which are related to the principal values of the respective tensors A and Q by

$$A_{xx} = (a - b + b') \qquad A_{yy} = (a - b - b') \qquad A_{zz} = (a + 2b) \quad (1)$$

$$Q_{xx} = q + q' \qquad Q_{yy} = -q - q' \qquad Q_{zz} = 2q. \quad (2)$$

Table 1. Superhyperfine interaction parameters of F centres, blue and red centres in KBr at 14 K. The experimental error is smaller than the last given digit. The angle θ describes the deviation of the tensor axes from the connection line neighbour nucleus centre. Values marked by — are zero by symmetry.

	Nucleus	Symmetry	a/h (MHz)	b/h (MHz)	b'/h (MHz)	θ_b (°)	q/h (MHz)	q'/h (MHz)	θ_q (°)
F centre	^{39}K	(100)	18.20	0.78	—	—	0.07	—	—
	^{81}Br	(110)	42.43	2.77	−0.13	0	0.07	0.01	0
	^{39}K	(111)	0.27	0.02	< 0.01	—	—	—	—
	^{81}Br	(100)	5.68	0.41	—	—	0.04	—	—
Blue centre	^{39}K$_\gamma$	(100)	35.61	1.04	—	—	0.23	—	—
	^{39}K$_\beta$	(100)	17.09	0.71	—	—	0.06	—	—
	^{39}K$_\alpha$	(100)	16.73	0.74	—	—	0.07	—	—
	^{81}Br	(110)	45.18	2.95	0.18	±5.7	0.53	−0.26	±92
	^{81}Br	(110)	38	2.7			0.4	−0.4	
	^{81}Br	(110)	37.69	2.54	−0.10	< ±2	0.09	−0.04	
	^{39}K	(111)	0.15	0.02	< 0.01	—	—	—	—
	^{1}H	(100)	−0.14	0.47	—				
Red centre	^{39}K$_\alpha$	(100)	20.92	0.84	—	—	0.06	—	—
	^{39}K$_\beta$	(100)	19.99	0.76	—	—	0.06	—	—
	^{39}K$_\gamma$	(100)	7.74	0.38	—	—	0.07	—	—
	^{81}Br	(110)	50.1	2.6		< ±2	0.07		< ±4
	^{81}Br	(110)	44.9	3.1	0.3	< ±2			
	^{81}Br	(110)							
	^{39}K	(111)	0.15	0.02	< 0.01				
	^{81}Br	(100)	6.37	0.43	—	—	0.07	—	
	^{1}H	(100)	0.15	0.19	—	—	—	—	—

The particular difficulty in the analysis of the ENDOR spectra was the simultaneous presence of isolated F centres and the red and blue centres causing the ENDOR spectra of all centres to be superimposed in the same frequency range, each having numerous ENDOR lines. Thus the angular dependence of each centre could not easily be separated from that of the others. As mentioned before, by creating and destroying red and blue F_H centres by the appropriate illumination, certain line assignments could be made. In order to identify more ENDOR lines of a particular centre double-ENDOR experiments were also performed and proved to be helpful (Niklas 1983). This special technique makes it possible to isolate ENDOR lines of particular centres or centre orientations (Niklas 1983, Möbius and Biehl 1979). The double-ENDOR technique uses the idea that only ligand spins of the same centre couple to the observed unpaired electron of that centre. This means, when measuring ENDOR,

the induction of an additional nuclear magnetic resonance (NMR) transition can only influence the intensity of a particular ENDOR line if the induced second ENDOR (NMR) transition takes place at a neighbour nucleus of the same centre. Therefore, in double-ENDOR experiments the intensity of a detected ENDOR line will generally change if a second NMR transition is induced at another neighbour of the unpaired electron. For these triple-resonance experiments we used ENDOR lines of nuclei with 'high symmetry' i.e. of those which are equivalent for the particular magnetic field orientation (Biehl *et al* 1975) in order to separate the three overlapping spectra. A comparison between a double-ENDOR spectrum measured on the highest ENDOR line for $B_0 \| [100]$ of the red centre (at 29.7 MHz, see figure 3) and a normal ENDOR spectrum is shown in figure 4. The normal ENDOR spectrum shows the typical situation where all three centres are observed simultaneously. In the double-ENDOR spectrum the different signs of the lines originate in the two electron spin states $m_s = +1/2$ and $m_s = -1/2$. A negative double-ENDOR line comes from $m_s = -1/2$, a positive one from $m_s = +1/2$ (Niklas *et al* 1983). These signs reflect the increase or decrease of the stationary ENDOR line intensities observed in the line at 29.7 MHz when inducing the 'second' NMR transitions. The quadrupole triplets of three subshells denoted as K_α, K_β, K_γ of the near ^{39}K neighbours of the red $F_H(OH^-)$ centre are indicated in the double-ENDOR spectrum. Due to the symmetry lowering by the presence of OH^- (see below) the six equivalent nearest neighbours of the F centre are not equivalent any more: there are now three 'subshells' (for the identification of shells K_α, K_β, K_γ see below and also see figure 5(*c*).

Table 2. SHF constants (MHz) of F and $F_H(OH^-)$ centres in KBr (at 14 K) and KCl (at 70 K).

		H			K_α	K_β	K_γ
		a/h (MHz)	b/h (MHz)	K	a/h (MHz)	a/h (MHz)	a/h (MHz)
KCl	F			20.72			
	$F_H(OH^-)$	0.02	0.28		20.72	21.79	13.68
KBr	F			18.20			
	blue $F_H(OH^-)$	−0.14	0.47		16.73	17.09	35.61
	red $F_H(OH^-)$	0.15	0.19		20.92	19.99	7.74

In figure 4, in the frequency range between 8 and 12 MHz, two subshells of the nearest ^{39}K of the red centre and the first shell ^{39}K lines of the isolated F centre are superimposed in the ENDOR spectrum. In the double-ENDOR spectrum only the ENDOR lines due to the ^{39}K nuclei of the subshells of the red centre appear (not all are marked in the double-ENDOR spectrum of figure 4).

The double-ENDOR technique was also used to perform a linewidth analysis of the nearest ^{39}K ENDOR lines. Feuchtwang (1962) showed in his early F-centre work that the indirect spin–spin coupling between equivalent nuclei broadens the ENDOR line in a characteristic way. In this context nuclei are equivalent if they have the same SHF and quadrupole tensors which also have the same orientation relative to the magnetic field. Therefore information about the centre symmetry can be obtained from an analysis of the measured ENDOR lineshapes. First the equivalent first-shell ^{39}K neighbours of the isolated F centre should be discussed.

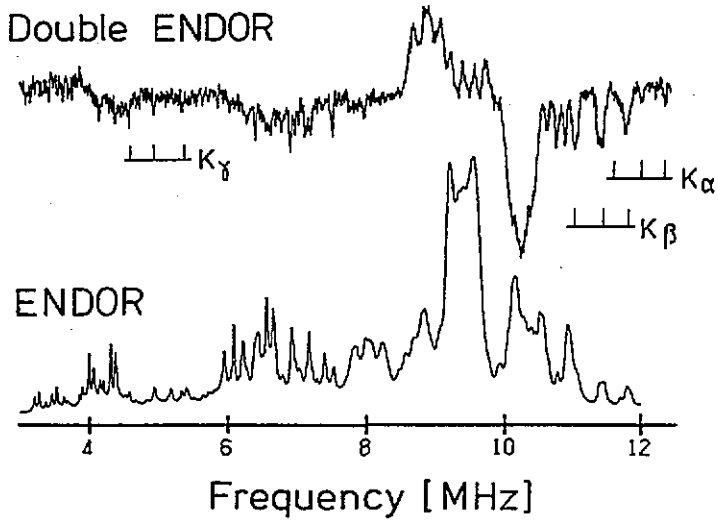

Figure 4. Double-ENDOR spectrum of the red centres in KBr measured on the ENDOR transition at 29.7 MHz compared with a conventional ENDOR spectrum. $B_0 \| [100]$, $T = 4.5$ K. ENDOR lines of the three subshells of the first shell of ^{39}K are marked.

In figure 5(*a*) for the magnetic field along ⟨100⟩ the interaction tensors of four neighbours are perpendicular and of two neighbours parallel to the magnetic field, thus four and two neighbours are equivalent, respectively. Similar considerations for the two possible static configurations of F_H centres with the OH^- residing on a (110) nearest-neighbour site or on a next-nearest (200) site lead to the following: for the OH^- in a (110) position there can be only three subshells with two equivalent potassium nuclei in each subshell, caused by a lattice relaxation due to the OH^- molecule (see figure 5(*b*)). But in the case of the OH^- in a (200) position again the four neighbours perpendicular to the $F - OH^-$) connection line are equivalent (for $B_0 \|$ the axis). In addition there are two non-equivalent nuclei (see figure 5(*c*)).

In figure 6(*a*) the spectrum of the four equivalent potassium neighbours of the isolated F centre ($B_0 \| [100]$) is shown, in figure 6(*b*) the double-ENDOR spectrum of the red centre for the same orientation, in figure 6(*c*) the ENDOR line due to two equivalent ^{39}K neighbours and in figure 6(*d*) the ENDOR line of a single ^{39}K nucleus of the red centre. The ENDOR linewidths are clearly largest for four equivalent nuclei and smallest for the single nucleus. The large linewidths of figure 6(*a*), (*b*) and (*c*) are due to the unresolved pseudodipolar coupling effects (Feuchtwang 1962). From the similar lineshapes of figure 6(*a*) and (*b*) it is concluded that the red centre must have four equivalent first-shell ^{39}K nuclei. This lineshape analysis clearly shows that the OH^- molecule in the red centre must reside in a (200) position, leading to a tetragonal symmetry of this defect.

Very similar investigations were performed on the blue centre. They show that the OH^- molecule is also in a (200) position in the blue centre and it also has tetragonal symmetry.

Therefore the first shell of six equivalent potassium neighbours of the isolated F centre splits into three new subshells after $F_H(OH^-)$ centre formation because of the reduction of symmetry. For both bistable configurations three subshells, with (100) axial symmetry of the SHF and quadrupole tensors for each subshell, were found.

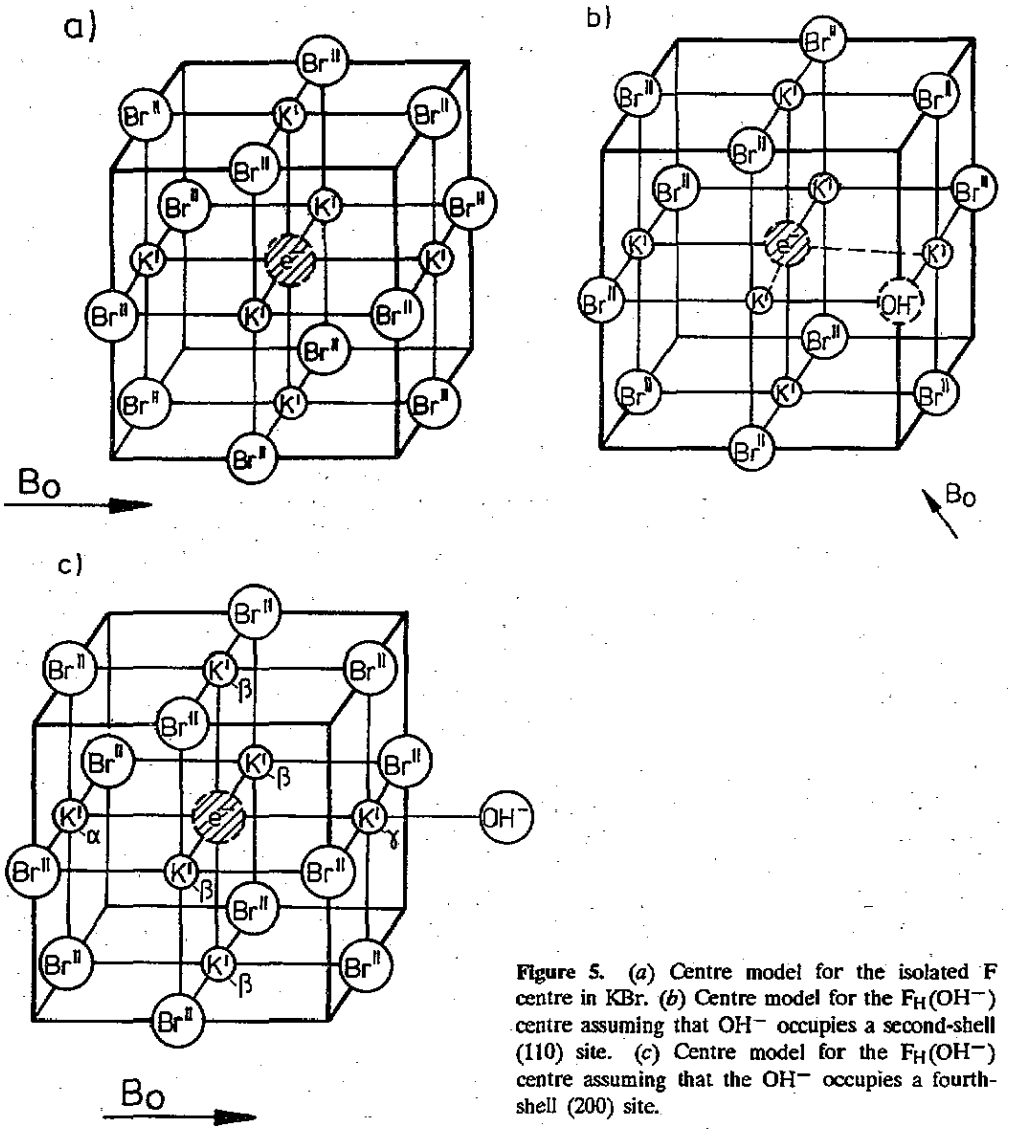

Figure 5. (*a*) Centre model for the isolated F centre in KBr. (*b*) Centre model for the $F_H(OH^-)$ centre assuming that OH^- occupies a second-shell (110) site. (*c*) Centre model for the $F_H(OH^-)$ centre assuming that the OH^- occupies a fourth-shell (200) site.

This result also indicates the tetragonal centre symmetry with the OH^- molecule on a fourth-shell bromine site for both the blue and the red centres. An OH^- molecule in the second shell, i.e. on a (110) site should cause a relaxation of the first-shell potassium nuclei from their sites on the ⟨100⟩ crystal axes. However, a deviation of the SHF tensor orientations from the axial (100) symmetry was not observed for any of the first-shell potassium nuclei.

ENDOR lines of the hydrogen nuclei in the OH^- molecule could also be identified. ENDOR transitions from the oxygen nuclei are not expected because of the low abundance of magnetic oxygen isotopes. Figure 7(*a*) shows the angular dependence of the hydrogen ENDOR line positions of the blue centre (measured in a K-band spectrometer at $B_0 = 892$ mT) for rotation of B_0 in a {001} plane. Figure 7(*b*) shows the corresponding ENDOR angular dependence of the hydrogen ENDOR transitions of

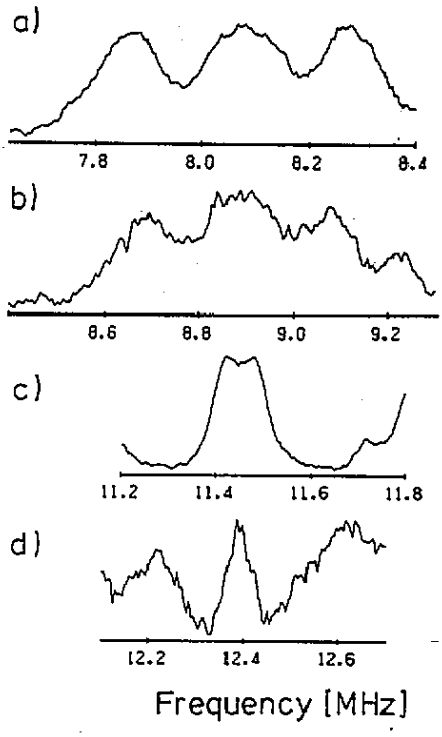

Figure 6. Comparison of observed ENDOR lineshapes of the red centre and the isolated F centre in KBr: (*a*) F centre: four equivalent K nuclei; (*b*) red centre: four equivalent K nuclei for B_0 parallel to the (F–OH^-) interconnection line; (*c*) red centre: two equivalent K nuclei for B_0 perpendicular to the (F–OH^-) interconnection line; (*d*) red centre: one single K nucleus (see also figure 5(*c*)).

the red centre (measured in an X-band spectrometer at $B_0 = 341$ mT). Both angular dependences show the typical pattern of nuclei with axial (100) symmetry (Seidel 1961, Spaeth *et al* 1992). The SHF constants are listed in table 1. There is no difference in the symmetry of the SHF tensors, but the values and signs of the isotropic and anisotropic SHF constants a and b differ markedly. For the red centre both SHF constants have the same sign and are assumed to be positive as is usual for F centres. In contrast, the two SHF constants of the hydrogen atoms in the blue centre have opposite signs. Because of the localized wavefunction of the F centre and also of the F_H centre the anisotropic constant b was chosen to be positive.

4. Dynamical properties of $F_H(OH^-)$ centres

It must be assumed that in the red configuration the OH^- dipoles have vibrations in the Br^- vacancy in addition to the known hydrogen stretch vibrations of the OH^- molecule. Experimental evidence for such vibrations comes from the observation of a temperature dependence of SHF constants. In KBr the ENDOR lines of the red centre could only be measured up to 20 K, which was not enough to measure the temperature dependence. However, the ENDOR lines of $F_H(OH^-)$ centres in KCl can be measured up to about 240 K. In KCl $F_H(OH^-)$ centres have similar optical properties and the same microscopic structure as the red centres in KBr (Jordan 1987). There are only minor quantitative differences.

A comparison of $F_H(OH^-)$ centres in KCl and the red centre in KBr shows that the SHF constants of both centres are very similar (table 2). The isotropic constants a for the hydrogens are positive, i.e. the OH^- axis is parallel to the OH^-–F centre

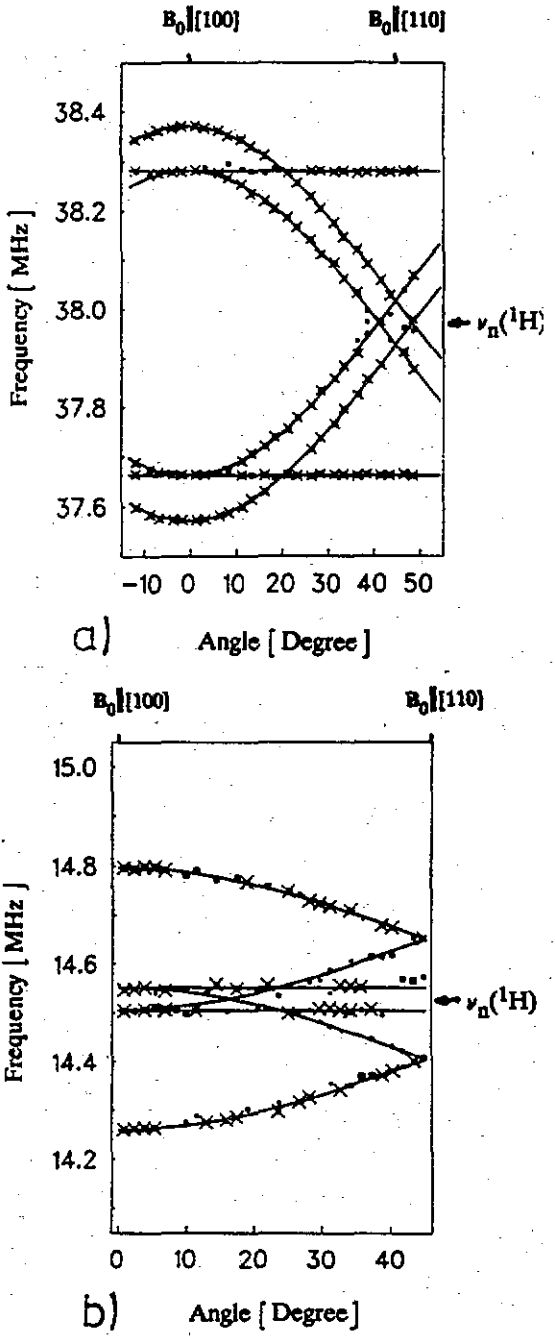

Figure 7. Angular dependences of the hydrogen ENDOR lines. The blue centre transitions (*a*) were measured in a K-band spectrometer (B_0 = 892 mT) and the red centre lines (*b*) in an X-band spectrometer (B_0 = 341 mT). The magnetic field was rotated in a (001) plane.

interconnection line (see below). One of the three potassium subshells of the red centre and the $F_H(OH^-)$ centre in KCl has a clearly lower SHF interaction compared to the first-shell potassium nuclei in the isolated F centre indicating an outward shift of the K_γ neighbours, making the anion vacancy larger. In KCl the K_γ nucleus was estimated to be shifted by about 11% outwards towards the OH^-; the hydrogen of the OH^- molecule is 6.9 Å away from the centre of the F electron (Jordan 1987).

There is no bistability in KCl, i.e. no blue $F_H(OH^-)$ centres were observed. We conclude that the structure of the $F_H(OH^-)$ centre in KCl is identical to that of the red centre in KBr, whereas the blue centre is a new configuration.

The ENDOR measurements performed on the $F_H(OH^-)$ centre in KCl showed a very strong temperature dependence of the SHF interaction of both the hydrogen in the OH^- molecule and of the K_γ nucleus, starting at very low temperatures. This indicates that the OH^- molecule and the K_γ nucleus vibrate in a rather shallow potential. In figure 8 the anisotropic SHF constant b of the hydrogen is plotted as a function of temperature; in figure 9 the isotropic constant a of the K_γ nucleus is shown. With increasing vibrational amplitude the overlap with the F centre wavefunction increases, which leads to larger SHF constants as seen in figures 8 and 9. The temperature dependence was analysed following the analysis of the temperature dependence of atomic hydrogen centres in alkali halides (Spaeth 1969, Hoentzsch and Spaeth 1978, 1979), in the approximation that for the lowest temperature range the validity of a harmonic potential for the vibrations can be assumed. From this crude analysis an activation energy of ~ 1.5 meV was obtained for the hydrogen atoms and ~ 1.8 meV for the K_γ nucleus. The vibrations show, however, a strong anharmonicity.

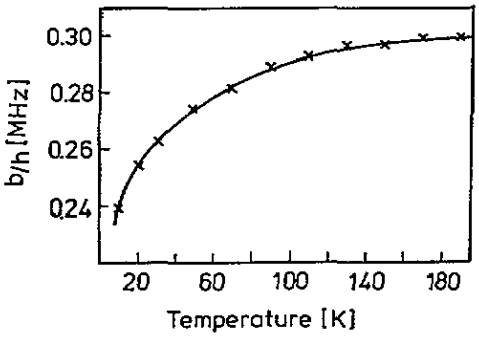

Figure 8. Temperature dependence of the anisotropic SHF constant b/h of the hydrogen atom in the red $F_H(OH^-)$ centre in KCl.

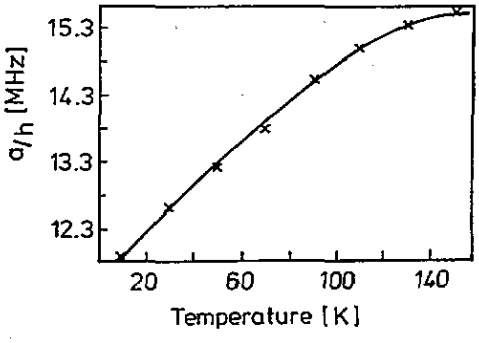

Figure 9. Temperature dependence of the isotropic SHF constant a/h of the K_γ nucleus in the red $F_H(OH^-)$ centre in KCl.

Since the space for the OH^- molecule is larger in KBr than in KCl it must be assumed that also in KBr there is a soft OH^- and K_γ vibration as was observed in KCl. One should expect that the vibration potential in KBr is softer than in KCl due to the larger anion vacancy space. Probably the vibration is also very anharmonic. It should be noted that in KCl and KBr doped with OH^- a soft OH^- vibration in the energy range of 37 cm^{-1} was observed in infrared absorption (Wedding and Klein 1969). This vibrational energy is of the same order of magnitude as the one observed for the $F_H(OH^-)$ centre. In $F_H(OH^-)$ centres the vibration is probably softened due to the nearby presence of the F centre electron instead of a Br^- ion.

5. Discussion

5.1. Centre models

From the axial symmetry along ⟨100⟩ axes of the interaction tensors of the six near

^{39}K nuclei as well as from the hydrogen atoms of the OH^- dipoles, it is clear that OH^- cannot occupy a second shell (110) site, but can only be on a (200) fourth shell site in both cases. Thus the question arises, why are the two configurations different and what is the difference? A key to the answer of this question is the discussion of the SHF interactions of the hydrogen atoms of both centres. The unusual result is that for the blue centre a has the opposite sign to b, while for the red centre both have the same sign. Following the usual method to explain the SHF constants by orthogonalizing the F centre wavefunction to the cores of the neighbour ions (Seidel and Wolf 1968), a negative sign of the isotropic SHF constant of hydrogen could not be explained if the OH^- molecular axis is parallel to the [100] axis connecting the F centre and the OH^- site. A negative sign can, however, be explained by exchange polarization effects, if the dipole axis of the OH^- molecule is orientated perpendicularly to the defect pair axis. In this case p_σ orbitals of oxygen are admixed into the F centre envelope function which are oriented parallel to the oxygen–F centre connection line. The hydrogen atom, however, is in a nodal plane of the p_σ orbitals which leads to a negative SHF constant (Adrian *et al* 1985).

In the free OH^- in KBr the dipole axes are oriented along ⟨100⟩ axes (Kapphan and Lüty 1973) and their reorientation rate between the ⟨100⟩ axes is 10^5 Hz (Kapphan 1974). A reorientation between the four equivalent orientations of the OH^- dipoles perpendicular to the [100] defect pair axis with a slow rate compared to the SHF interaction frequencies would reduce the symmetry of the ENDOR spectra such that one would not observe the (100) symmetry of the hydrogen and K_γ SHF tensors. The tetragonal centre symmetry and the axial (100) symmetry of the hydrogen SHF tensor can be understood if the OH^- dipole tunnels between the four equivalent ⟨100⟩ orientations perpendicular to the defect pair axis with a rate that is fast compared to the SHF interaction frequencies. The presence of the F centre apparently leads to a higher OH^- tunnelling rate in the plane perpendicular to the defect pair axis compared to the free OH^- molecule. The lattice dressing effects which hinder the OH^- reorientation are obviously smaller for the pair centres (Kapphan 1974).

In figure 10 the proposed structure models of both bistable configurations are sketched. The unpaired F electron is represented by the hatched circle which has the size of the missing Br^- ion. The other ions are sketched according to their ionic radii. The distance R of the hydrogen atom from the centre of the F centre can be estimated from the analysis of the anisotropic SHF constant b, which is explained by the classical point dipole–dipole interaction (Spaeth *et al* 1992, Seidel and Wolf 1968) with

$$b = \mu_0 g_I \beta_n g_e \beta_e / (4\pi R^3). \tag{3}$$

In the blue centre the hydrogen atom is 5.5 Å away from the centre of the F electron on the basis of this estimate. In the red centre the hydrogen atom is 7.4 Å away from the F centre. This implies that the oxygen in the OH^- molecule must point towards the F centres such that the hydrogen atom is next to the potassium nucleus in the ninth shell (see figure 10).

For each $F_H(OH^-)$ configuration there is one ^{39}K subshell with a significantly different isotropic SHF interaction from that of the isolated F centre. These potassium nuclei are labelled K_γ (see figure 5(*c*)). They must be placed between the F centre and the OH^- molecule. The isotropic SHF constant a for the K_γ nucleus in the blue centre is nearly twice as high as that of the first-shell K neighbours of the isolated F

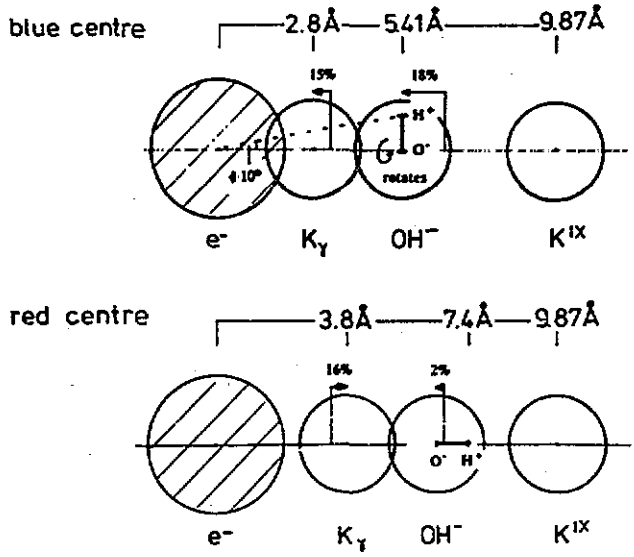

Figure 10. Structure models of the blue and red $F_H(OH^-)$ centres in KBr.

centre. In order to estimate the isotropic SHF interaction parameters of the $F_H(OH^-)$ centres in KBr the wavefunctions of Clementi and Roetti (1974) were used for the free lattice ions. As an envelope function, Bennett's (1968) function for the F centre in KCl was taken and orthogonalized to the K^+ and Br^- ion cores (Gourary and Adrian 1957):

$$\psi = (7\pi)^{-1/2}\beta^{3/2}(1+\beta r)\exp(-\beta r) \tag{4}$$

with

$$\beta = 10.77\ \mathrm{nm}^{-1}.$$

Bennett's envelope function yields also good results in KBr. For the isolated F centre we could explain with it the SHF interaction constants of the first two shells within 5% of the experimental values. Assuming that the OH^- ion in the fourth shell will not change the F-centre wave function very much, we took it to estimate the position of the K_γ nuclei using the experimental values (table 1), again with the orthogonalized envelope function method. In the blue centre K_γ is relaxed by about 15% of the normal distance towards the F centre; in the red centre it is shifted by approximately 16% outwards towards the OH^- molecule (see figure 10). The isotropic SHF constants of K_α and K_β differ less than 10% from the F-centre value. This shows that the major effect on the SHF interactions of the nearest K is the position of the OH^- molecule with respect to the F electron. K_β is for both centres the subshell with four equivalent K nuclei which was identified by observing the line broadening because of pseudodipolar coupling. K_α is the remaining single nucleus opposite K_γ (see figure 5(*c*)).

On the basis of these structure models the peak energies of the absorption bands can be qualitatively explained. In the blue centre the K_γ nucleus is shifted 'into' the F centre. Therefore the potential box for the F electron becomes smaller, such that

the absorption band of the blue centres will shift to higher energies compared to the F centre according to the Mollwo–Ivey relation (Fowler 1968). On the other hand the space available for the F electron in the red centre becomes larger. This results in a shift of the red centre absorption band to lower energies compared to the F band.

5.2. Thermal bistability

The striking difference between $F_H(OH^-)$ centres in KCl and KBr is the fact that in KBr there are two configurations of the fourth-shell OH^- impurity, one dominant at high temperatures and one dominant at low temperatures, whereas in KCl only one configuration is observed. Although we were not able to measure the red centres above 20 K with ENDOR, probably due to dynamical effects on the nuclear spin lattice relaxation times, we think that the high-temperature centre has the structure of the red centre. The absorption of the red centre at low temperatures, which can only be measured after low-temperature optical switching, is where it is expected when extrapolating from the high-temperature position with the typical F-centre temperature shifts (Baldacchini *et al* 1989). The same temperature shift was also observed for the $F_H(OH^-)$ centres in KCl (Jordan 1987). The reason why the blue centre is only observed in KBr and not in KCl may have to do with the larger space available for the OH^-. Preliminary ODESR and ENDOR experiments in KI showed also the existence of the same bistability with similar properties of the blue and red centres as in KBr.

Our observations can be summarized in a diagram where the internal energy curves are schematically plotted versus a configuration coordinate, which we identified with the orientation of the OH^- dipole parallel or perpendicular to the defect pair axis (figure 11). At temperatures below 5 K down to 3.6 K, the lowest temperature available, blue and red centres were observed in the dark. The number of red centres decreases and that of blue centres increases upon cooling. At low temperatures the number of red centres is very small. For the free OH^- molecules the barrier for reorientation is ~ 0.1 eV (Kapphan 1974). Assuming that the presence of the F centre does not change the order of magnitude of the barrier height, then the occupation changes of the blue and red centres can only be explained by phonon assisted tunnelling. At 10–15 K both centres are present in numbers of approximately the same order of magnitude according to ENDOR. Above 40 K the red centre prevails as seen from the shifts of the optical absorption bands. Its energy is now lowest.

It remains to discuss why such a temperature dependent bistability should occur. It is hard to see that the thermal expansion of the lattice alone could be responsible for the bistability. Comparison of KCl on the one hand and KBr and KI on the other hand would rather favour the stability of the blue configuration at high temperatures, where the space for the OH^- is larger than at low temperatures, if the temperature expansion was the reason. Tentatively we propose that the thermal bistability is due to the entropy associated with both defects. Such a theoretical model was suggested by Hamilton *et al* (1988) to describe a metastability observed by deep-level transient spectroscopy (DLTS) of an unknown defect in silicon. Instead of discussing the internal energy one has to consider the Gibbs free energy which is given by

$$G = H - TS \tag{5}$$

where H is the configuration enthalpy, T the temperature and S the entropy. For $T = 0$ there is no influence of the entropy term. Apparently the value of G is lower at

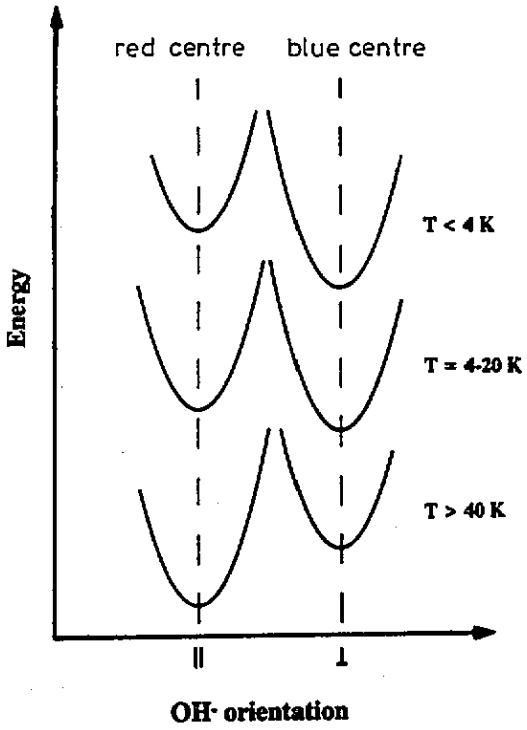

Figure 11. Schematic representation of the internal energy as a function of the OH^- orientation as 'configuration' coordinate for various temperatures.

$T = 0$ for the blue centre than for the red centre. If the entropy associated with each defect was constant as a function of temperature, G for the blue centre would always remain lower than for the red centre and consequently only the blue configuration would be occupied, or would at least be preferentially occupied according to the Boltzmann statistics. The entropy is given by

$$S = k_B \ln W \tag{6}$$

where W represents the number of microscopic states associated with the observed configuration. A difference in S for the two configurations would change G as a function of temperature. If the value of S associated with the red centre is larger than that associated with the blue centre, i.e. $\Delta S(S_{red} - S_{blue}) > 0$, than for a sufficiently high temperature

$$\Delta G = G_{red} - G_{blue} = (H_{red} - H_{blue}) - T(S_{red} - S_{blue}) < 0. \tag{7}$$

This means that at a sufficient high temperature G_{red} can be below G_{blue}, i.e. the red centre becomes the more stable configuration as we have observed. In a crude estimate we propose that the entropy difference of the two configurations is associated with the dynamical properties of the OH^- dipoles. We also assume that $\Delta H = (H_{red} - H_{blue})$ is small and not temperature dependent. ΔH must be orders of magnitude below the barrier height between the two configurations. It is probably only of the order of a few kelvin according to our observations of the tunnelling reorientations at low temperatures. The entropy of the red centre is assumed to be mainly associated with the soft vibration of the OH^- molecule and the K_γ nucleus. It is a function of temperature and increases with increasing temperature. From the

observation that in the blue centre the K_γ nucleus and the OH^- are compressed towards the F centre we assume that no soft OH^- vibration exists and that its entropy factor is given by the four equivalent orientations of the OH^- molecules perpendicular to the centre axis. Figure 12 shows the calculated entropy in units of k_B assuming different harmonic potentials of the OH^- and K_γ vibrations in the red centre compared to ln 4 for the blue centre. It is seen that for vibrational energies of the order of 1 meV at low temperatures the entropy of the red centre already exceeds that of the blue centre. This entropy factor can therefore qualitatively explain the stability of the red configuration at higher temperature according to equation (7) if the entropy exceeds ΔH. From the optical absorption experiments we know that the red centre is more stable at temperatures above about 40 K. For 40 K and assuming 1 meV vibrational energy the entropy term $T\Delta S$ is more than an order of magnitude larger (about 125 K) compared to a value for this term at 4 K (about 4 K). A vibrational OH^- energy of 1.5 meV was observed in KCl and it can be assumed to be of the same order of magnitude in KBr, where it is probably considerably smaller. The strong anharmonicity observed would increase the entropy associated with these vibrations. Therefore we propose that the consideration of the entropy factor associated with the two $F_H(OH^-)$ configurations can explain qualitatively the observed thermal bistability.

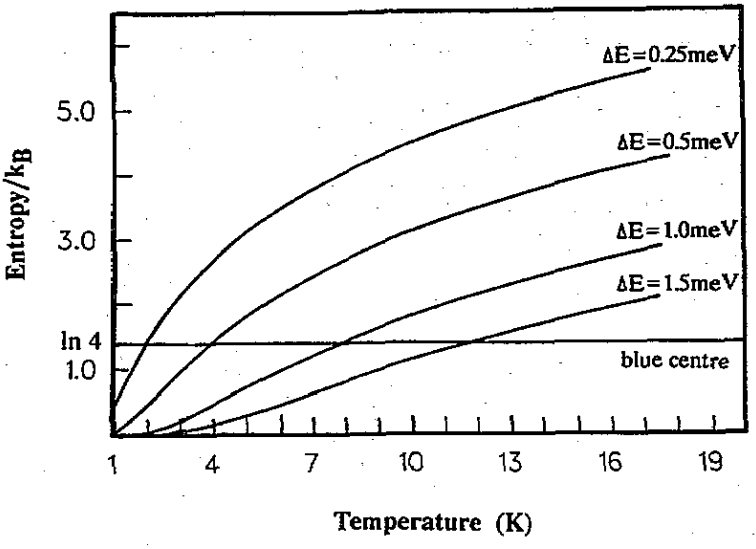

Figure 12. Calculated entropy for the red and blue centres in KBr.

To our knowledge this is the first case where for a precisely known microscopic defect structure it has been demonstrated that the entropy factor associated with the defect may be important for the centre stability.

Acknowledgments

One of the authors (FL) was supported by the NSF Grant DMR 87-06416 and ONR N 00014-90J-1841. Helpful discussions with Dr A M Stoneham are gratefully acknowledged by one of us (JMS).

References

Adrian F J, Jette A N and Spaeth J-M 1985 *Phys. Rev.* B **31** 3923
Ahlers F J 1985 *Doctoral Thesis* University of Paderborn
Ahlers F J, Lohse F, Spaeth J-M and Mollenauer L F 1983 *Phys. Rev.* B **28** 1249
Baldacchini G, Botti S, Grassano U M, Gomes L and Lüty F 1989 *Europhys. Lett.* **9** 735
Bennett H S 1968 *Phys. Rev.* **169** 729
Biehl R, Plato M and Möbius K 1975 *J. Chem. Phys.* **63** 3515
Clementi E and Roetti C 1974 *At. Data Nucl. Data Tables* **14** 177
Feuchtwang T E 1962 *Phys. Rev.* **126** 1616, 1628
Fowler W B 1968 *Physics of Color Centres* ed W B Fowler (New York: Academic) ch 2, p 53
Gomes L and Lüty F 1984 *Phys. Rev.* B **30** 7194
Gourary B S and Adrian F J 1957 *Phys. Rev.* **105** 1180
Hamilton B, Peaker A R and Pantelides S T 1988 *Phys. Rev. Lett.* **61** 1627
Hoentzsch Ch and Spaeth J-M 1978 *Phys. Status Solidi* b **88** 581
—— 1979 *Phys. Status Solidi* b **94** 497
Hofmann D M, Meyer B K, Lohse F and Spaeth J-M 1984 *Phys. Rev. Lett.* **53** 1187
Jordan M 1987 *Diplomarbeit* University of Paderborn
Jordan M, Söthe H, Spaeth J-M and Lüty F 1988 *Proc. Int. Conf. on Defects in Insulating Crystals (Parma, Italy, 1988)* p 11
Kapphan S 1974 *J. Phys. Chem. Solids* **35** 621
Kapphan S and Lüty F 1973 *J. Phys. Chem. Solids* **34** 969
Möbius K and Biehl R 1979 *Multiple Resonance Spectroscopy* ed M M Dorio and J H Freed (New York: Plenum) pp 475–507
Niklas J R 1983 *Habilitationsschrift* University of Paderborn
Niklas J R, Bauer R U and Spaeth J-M 1983 *Phys. Status Solidi* b **119** 171
Seidel H 1961 *Z. Phys.* **165** 218
Seidel H and Wolf H C 1968 *Physics of Color Centres* ed W B Fowler (New York: Academic) pp 537–624
Söthe H, Spaeth J-M and Lüty F 1990 *Rev. Solid State Sci.* **4** 499
Spaeth J-M 1969 *Phys. Status Solidi* **34** 171
Spaeth J-M, Niklas J R, Bartram R H 1992 *Structural Analysis of Point Defects in Solids: Introduction to Multiple Magnetic Resonance Spectroscopy* (Heidelberg: Springer)
Van Doorn C Z 1961 *Rev. Sci. Instrum.* **32** 755
Wedding B and Klein M V 1969 *Phys. Rev.* **177** 1274